

Proceeding Paper

Camellia-sinensis- and Cocos-nucifera-Derived Gold Nanoparticles for Treatment of Infections Caused by Antibiotic-Resistant *Staphylococcus aureus*[†]

Saman Anwar¹, Sidra Altaf^{2,*} , Muhammad Saif Ur Rehman Babar¹, Bilal Aslam¹, Humaira Muzaffar³ and Arslan Iftikhar³ 

¹ Institute of Physiology and Pharmacology, University of Agriculture Faisalabad, Faisalabad 38000, Pakistan; samanwar3933@gmail.com (S.A.); drsaifbabar@gmail.com (M.S.U.R.B.); bilal.aslam@uaf.edu.pk (B.A.)

² Department of Pharmacy, University of Agriculture Faisalabad, Faisalabad 38000, Pakistan

³ Department of Physiology, Government College University Faisalabad, Faisalabad 38000, Pakistan; dochumairamuzaffar@gcuf.edu.pk (H.M.); arslaniftikhar@gmail.com (A.I.)

* Correspondence: sidra.altaf@uaf.edu.pk

† Presented at the 4th International Online Conference on Nanomaterials, 5–19 May 2023; Available online: <https://iocn2023.sciforum.net>.

Abstract: The development of bacterial resistance toward existing antibiotics is a universal problem for human and animal health as well as for food security. In an attempt to overcome this problem, nanotechnology has contributed in the form of nanoformulations. However, these are associated with risks and drawbacks including environmental toxicity, cell injury, issues of high production cost and the scarcity of active ingredients. On the other hand, the green synthesis of nanoformulations via biological methods is a simple, innovative, ecofriendly, cost effective and advanced approach for the treatment of lethal infections caused by multidrug-resistant organisms such as *staphylococcus aureus*. About 30% of humans are asymptomatic carriers of *S. aureus* in their upper respiratory tract. Clinical diseases caused by *S. aureus* infections range from mild to severe and may be manifested in the form of pneumonia, osteomyelitis, skin and deep tissue infections. Here, we prepared plant-mediated gold nanoparticles from *Camellia sinensis* and *Cocos nucifera*. The green biocompatible nanoparticles were characterized by using UV-Visible spectroscopy (UV-Vis. spectroscopy), X-ray diffraction (XRD), scanning electron microscopy (SEM), transmission electron microscopy (TEM), dynamic light scattering (DLS) and Fourier transform infrared spectroscopy (FTIR). Moreover, these green gold nanoparticles were investigated for their antimicrobial activity by checking their minimum inhibitory concentrations (MICs). We found that the newly developed bio-nanoparticles showed strong activity against the multidrug-resistant *Staphylococcus aureus*.

Keywords: gold nanoparticles; green nanotechnology; *Camellia sinensis*; *Cocos nucifera*; antibiotic resistant; ampicillin



Citation: Anwar, S.; Altaf, S.; Babar, M.S.U.R.; Aslam, B.; Muzaffar, H.; Iftikhar, A. *Camellia-sinensis*- and *Cocos-nucifera*-Derived Gold Nanoparticles for Treatment of Infections Caused by Antibiotic-Resistant *Staphylococcus aureus*. *Mater. Proc.* **2023**, *14*, 67. <https://doi.org/10.3390/IOCN2023-14469>

Academic Editor: José Luis Arias Mediano

Published: 5 May 2023



Copyright: © 2023 by the authors. Licensee MDPI, Basel, Switzerland. This article is an open access article distributed under the terms and conditions of the Creative Commons Attribution (CC BY) license (<https://creativecommons.org/licenses/by/4.0/>).

1. Introduction

Staphylococcus aureus is a Gram-positive bacterium that occurs as a common member of microbiota of the body and is usually present in clinical sites across the world [1]. About 30% of humans are asymptomatic carriers of *S. aureus* in their upper respiratory tract [2]. Additionally, around 80% of invasive *S. aureus* infections arise from a strain of hosts' microflora [3]. Clinical diseases caused by *S. aureus* infections range from mild to severe and may be manifested in the form of pneumonia, osteomyelitis, skin and deep tissue infections. The treatment of *S. aureus* infections is becoming increasingly difficult due to antibiotic resistance. Antibiotic resistance does not only harm human health but also affects the economy of developing and developed countries [4]. Every year, 95,000 invasive multidrug-resistant *S. aureus* infections occur in the United States alone [2].

According to WHO assessments, infections of multidrug-resistant *S. aureus* account for more than 25,000 deaths each year, which will grow to a whopping 10 million in 2050 [4]. An extremely virulent antibiotic-resistant strain of *S. aureus* is the ampicillin-resistant strain [5]. Several pharmaceutical formulations such as penicillins, sulfonamides, tetracyclines and glycopeptides are available for the treatment of *S. aureus* infections. These antibiotics show several side effects and are expensive, especially in developing countries such as Pakistan, India and Bangladesh. Most importantly, resistance is developing against these potent antibiotics. To overcome these effects, bionanoformulations have been designed.

Nanotechnology is a developing division of pharmaceutical science wherein the particles are restricted to the nanosize [6,7]. Nanoparticles prepared via various physical and chemical methods are not highly recommended due to their toxic effects; however, those prepared via biological methods are preferred due to beneficial features including cost-effectiveness, biocompatibility, biodegradability and eco-friendliness, and green synthesis affords a good source for high productivity and purity, because toxic chemicals and hazardous substances are avoided in the manufacturing process of nanoparticles [8].

Metallic nanoparticles are used for different pharmaceutical, agricultural and medicinal applications [9]. Their essential features, such as physicochemical properties and electronic and optics properties, can be fine-tuned by altering the characterization of nanoparticles, for example, regarding their aspect format, size and shape [10]. Numerous metals and their oxides are being used in biological systems as nanoparticles because of their easy production and promising optical properties [11]. Moreover, metals derived from plants have extreme potential to improve human health if applied in the agricultural, food and biomedical fields [12].

Green synthesis is the amalgamation of nanoparticles with plants and their metabolites. In green nanotechnology, biological substances are utilized to formulate nanoparticles for pharmaceutical purposes and other applications. The synthesis of nanoparticles via green biological methods is highly beneficial because the method has the ability to curtail the toxic effects of nanoparticles [6]. Gold nanoparticles synthesized via green nanotechnology are biocompatible and biodegradable, as these nanoparticles are obtained from natural plant sources, and no toxic chemical agent is consumed during preparation [13]. Green nanoparticles are economical as compared to conventional brands of drugs.

Antibacterial agents are basically significant in decreasing the load of infectious disorders. The development and spread of multidrug-resistant strains of pathogenic bacteria represent a significant and lethal public health hazard, as there are few or sometimes even no effective antibacterial agents accessible for the infection produced by resistant pathogenic bacteria [14]. There is an ultimate need to develop a potent therapeutic agent for the treatment of such lethal pathogenic infections. We prepared and characterized gold nanoparticles from CSE and CNW and investigated the newly developed nanodrug against deadly *S. aureus* infections.

2. Materials and Methods

Preparation of *Camellia sinensis* extracts (CSEs):

Here, 1 g of *Camellia sinensis* leaves was added to 50 mL of boiling water, the extract was filtered, and then the leaves were stirred with the help of a magnetic stirrer for 30 min [10].

Preparation of Tetra chloro auric acid solution:

A total of 3.9 mg of tetra chloro auric acid was weighed and mixed with 100 μ L of deionized water.

Preparation of gold nanoparticles via CS plant:

Camellia sinensis extract (9.9 mL) was placed in a beaker, and 3.9 mg of tetra chloro auric acid was added in 100 μ L of deionized water. This solution was stirred with the help of a magnetic stirrer for 15 min. The color of this solution initially changed from pale yellow to a purple red color, and this indicated the formation of gold nanoparticles. Additionally, this solution was mixed for 20 min.

Preparation of gold nanoparticles via CN plant:

Cocos nucifera water (9.9 mL) was placed in a beaker, and 3.9 mg of tetra chloro auric acid was added in 100 μ L of deionized water. This solution was stirred with the help of a magnetic stirrer for 30 min. The color of this solution initially changed from pale yellow to a purple red color, and this indicated the formation of gold nanoparticles. Additionally, this solution was mixed for 20 min. The preparation of green gold nanoparticles from *Camellia sinensis* and *Cocos nucifera* is summarized in Figure 1.

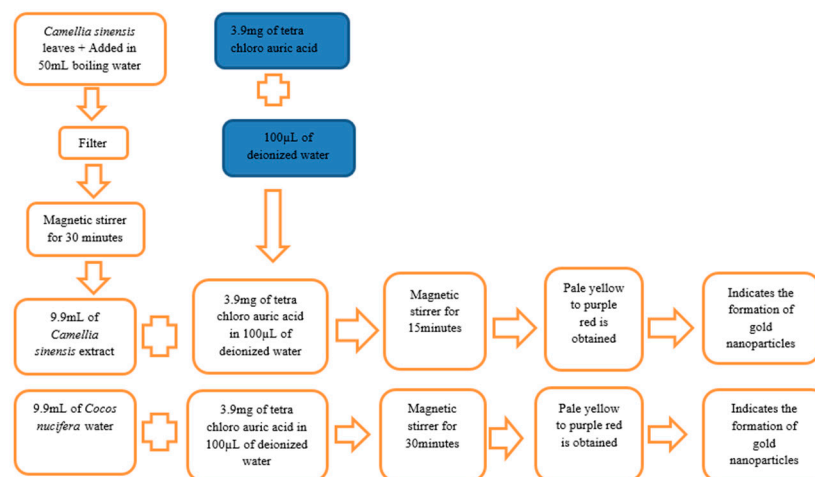


Figure 1. Summary of preparation of gold nanoparticles from *Camellia sinensis* and *Cocos nucifera*.

Dynamic light scattering:

Dynamic light scattering (DLS) was used to define the size dispersal profile of the gold NPs.

UV-Visible spectroscopy:

UV-Visible spectroscopy (UV-Vis spectroscopy) was used to determine the absorbance of the gold nanoparticles.

Fourier transform infrared spectroscopy:

Fourier transform infrared spectroscopy (FTIR) was used to provide information on the chemical composition and physical state of the gold NPs.

Scanning electron microscopy:

Scanning electron microscopy (SEM) was used to produce images of a sample by scanning the surface with a focused beam of electrons.

Transmission electron microscopy:

Transmission electron microscopy (TEM) (200 kV) was used to check the images of the gold NPs.

Energy-dispersive X-ray spectroscopy:

Energy-dispersive X-ray spectroscopy (XRD) was used to determine the crystallographic structure of the nanoparticles.

Antimicrobial activity:

The zone of inhibition was calculated using the well diffusion method on an agar plate. The pathogenic bacteria *Staphylococcus aureus* was grown overnight at 4 °C on Mueller Hinton agar plates. Each bacterium was grown on its own sterile Mueller Hinton agar plate in this process. Using sterile cotton swabs, pathogenic bacteria were coated on the agar plate, and these plates were dried. A sterile well cutter (6 mm in diameter) was used to drill wells in each agar plate. The nanoparticle suspension was poured into the wells. For full diffusion, these plates were placed for 1 h and then incubated at 37 °C for 1 day, and the diameter of the inhibitory zones was measured in mm [15].

Minimum inhibitory concentration (MIC):

A standard inoculum (10^5 CFU/mL) for the determination of the MICs was prepared using the Broth Micro Dilution method. A microtitration plate with 96 wells was filled

with nutrient broth. Leaving one positive control and one negative control, serial two-fold dilutions of gold nanoparticles in concentrations ranging from 3.9 mg/ μ L, 10 mg/ μ L, 30 mg/ μ L and 50 mg/ μ L with adjusted bacterial concentrations were used to determine the MICs. This experiment incorporated a positive control with a nutrient broth medium and inoculum and a negative control with a nutrient broth medium. The plate was incubated at 37 °C and observed for 24 h. Optical density (OD) values before and after incubation were measured at a 625 nm wavelength using a spectrophotometer. The net OD value was determined and compared with the cutoff value to find the minimum inhibitory concentration of these preparations of gold nanoparticles [16].

3. Results

3.1. Characterization of Gold Nanoparticles

Physical appearance:

The preparation of gold nanoparticles is commonly confirmed by color identifications. Through this experimentation, the appearance of a purple-red-color suspension from the initial pale yellow color showed the formation of gold nanoparticles mediated by CSE, and the appearance of the purple-red-color suspension from the CNW showed the formation of gold nanoparticles mediated by CN plants. The preparation of CSNp and CNNp is shown in Figures 2 and 3.

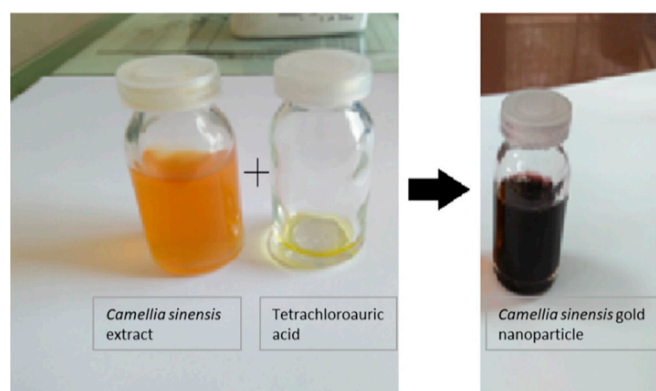


Figure 2. Gold nanoparticles prepared using *Camellia sinensis* plant.

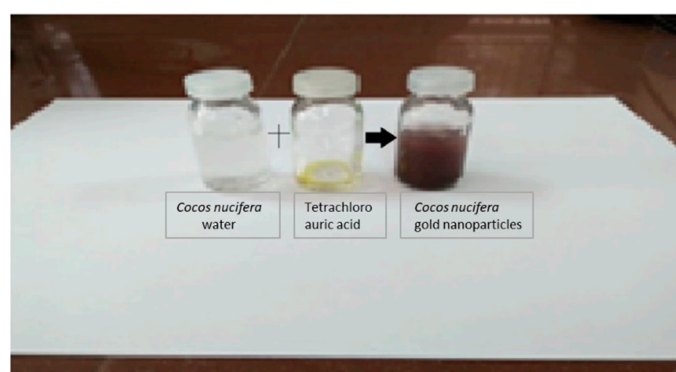


Figure 3. Gold nanoparticles prepared using *Cocos nucifera* plant.

Zeta size and Zeta potential:

Zeta size gives an estimate of the mean size of particles and their poly dispersity index (PDI). The average zeta size of CSNp was 41.61 nm, and for CNNp, it was 34.12 nm. The zeta sizes of the nanoparticles are given in Table 1, along with the zeta scan results in Figure 4a,b. The zeta potential of CSNp was -16.52 mV, and for CNNp, it was -14.61 mV. The zeta potential values of the nanoparticles are given in Table 1, along with the zeta scan results in Figure 5a,b.

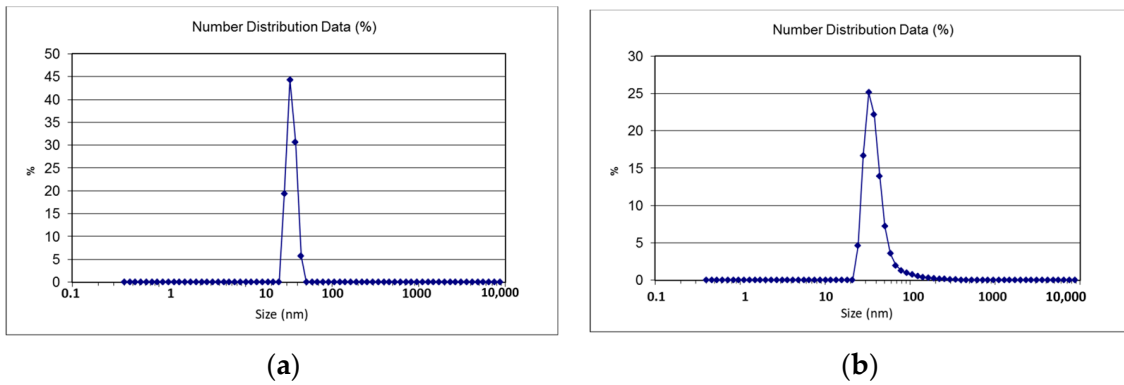


Figure 4. (a) Zeta size of CSNp; (b) zeta size of CNNp.

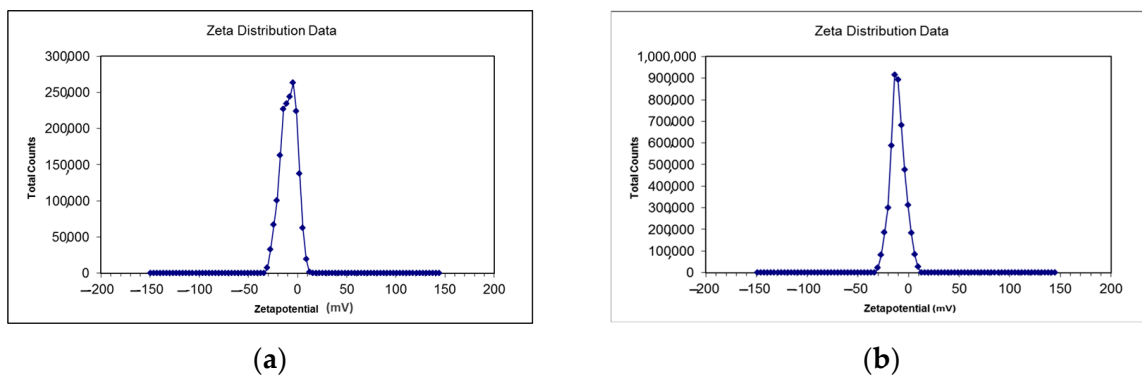


Figure 5. (a) Zeta potential of CNNp; (b) zeta potential of CSNp.

Table 1. Zeta size and zeta potential of CSNp and CNNp.

Formulations	Z-Average (nm)	PDI	Zeta Potential
CSNp	41.61	0.245	-16.52
CNNp	34.12	1	-14.61

3.2. Fourier Transform Infrared Spectroscopy

CSE and CSNp both had the same peaks, which confirmed the preparation of gold nanoparticles. CNW and CNNp both had the same peaks, which confirmed the preparation of gold nanoparticles via coconut water. These graphs are shown in Figure 6a,b.

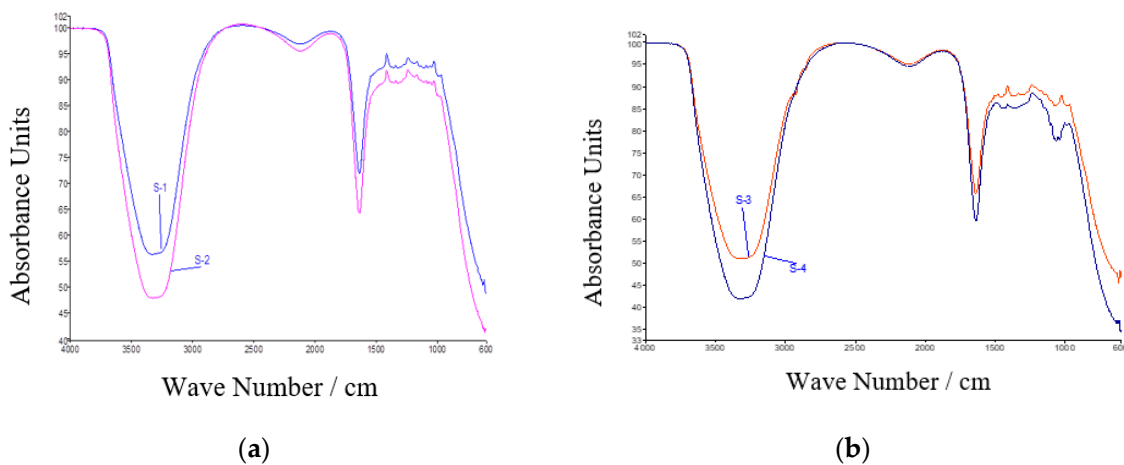


Figure 6. (a) S-1: CSE; S-2: CSNp; (b) S-3: CNW; S-4: CNNp.

3.3. Scanning Electron Microscopy

Scanning electron microscopy (SEM) presented images of the gold nanoparticles. SEM showed the morphology of the gold nanoparticles prepared from CSE and CNW had spherical shapes. SEM images are shown in Figure 7a,b.

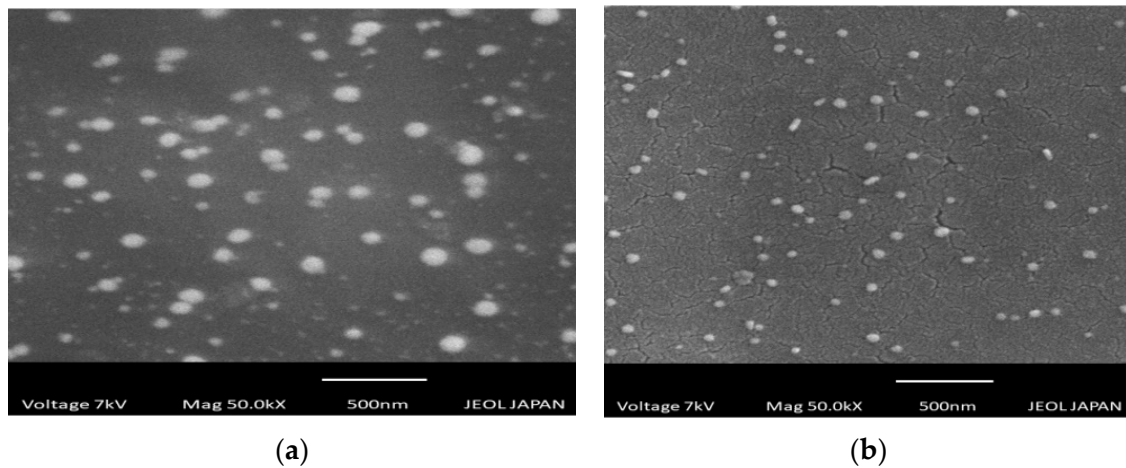


Figure 7. (a) SEM images of CNNp; (b) SEM images of CSNp.

3.4. Transmission Electron Microscopy

Transmission electron microscopy (TEM) was used to present images of the gold nanoparticles. TEM provided highly magnified images of the nanoparticles prepared from CSE and CNW. TEM also magnified the images up to 2 million times. The TEM images are shown in Figure 8a,b.

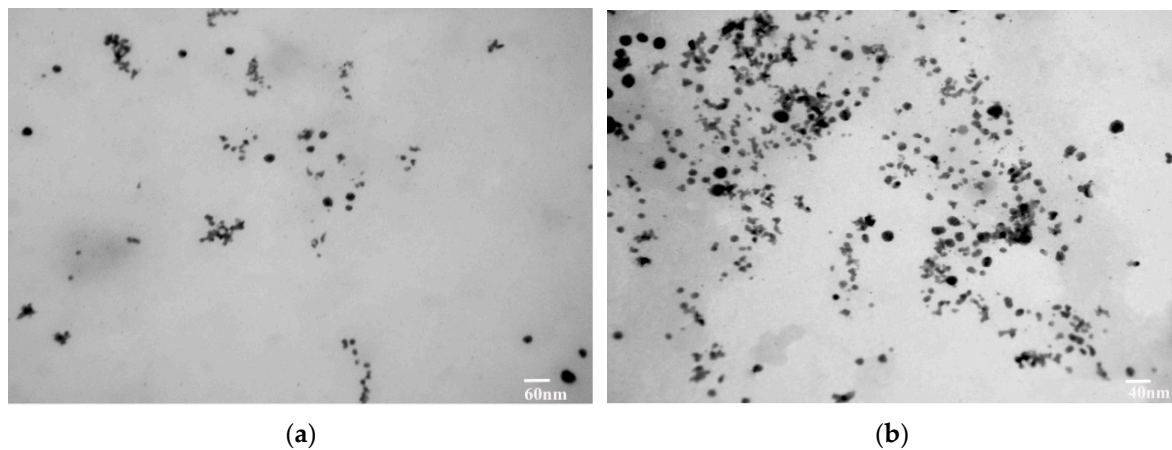
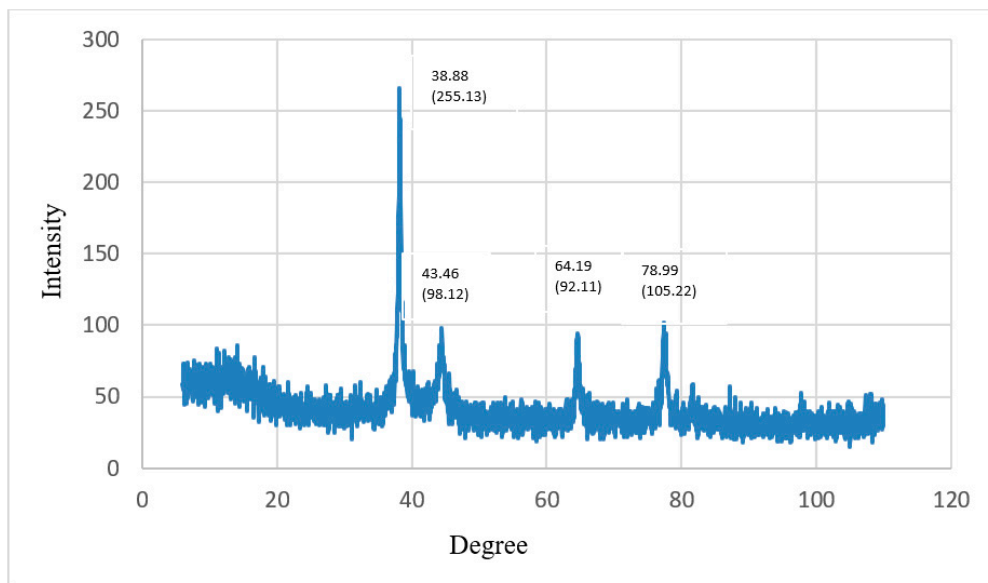


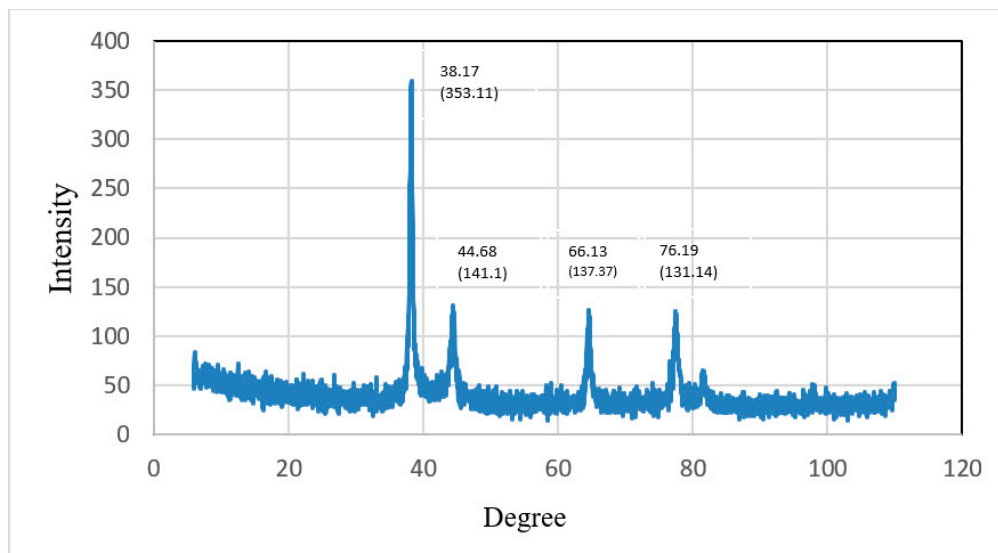
Figure 8. (a) TEM analysis of CSNp; (b) TEM analysis of CNNp.

3.5. Energy-Dispersive X-ray Spectroscopy

Energy-dispersive X-ray spectroscopy (XRD) was used to determine the crystallographic structure of the nanoparticles. XRD represented the crystalline nature of the gold nanoparticles prepared from CSE and CNW. The diffraction peaks of CSNp were observed at 38.17° , 44.66° , 66.13° and 76.19° , representing the intensities of (353.11), (141.1), (137.37) and (131.14). The diffraction peaks of CNNp were observed at 38.88° , 43.46° , 64.19° and 78.99° , representing the intensities of (255.13), (98.12), (92.11) and (105.22), which describe the crystalline structures of gold nanoparticles. XRD graphs are shown in Figure 9a,b.



(a)

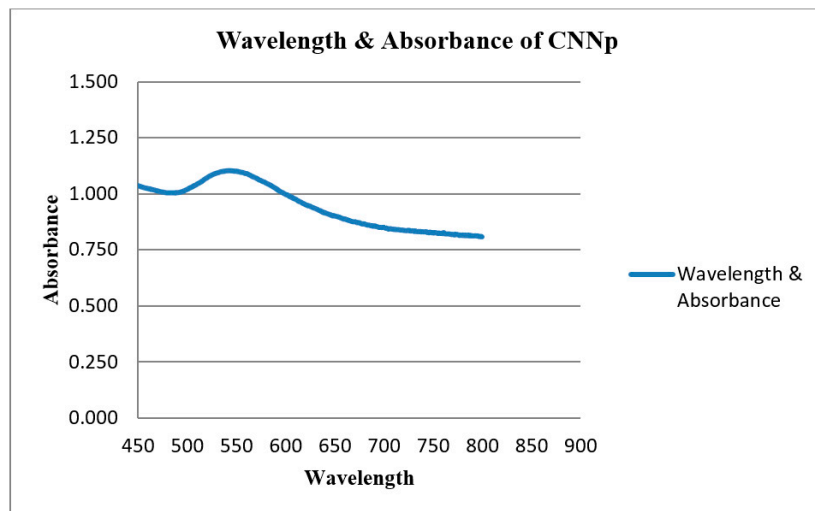


(b)

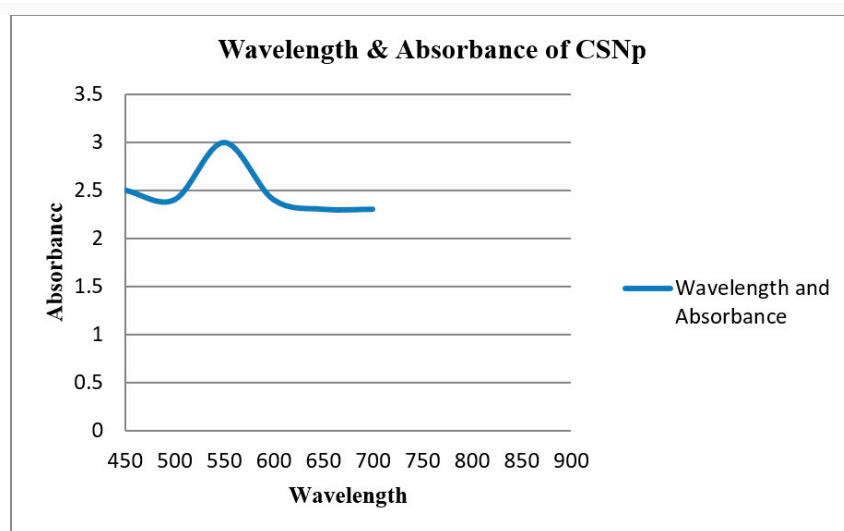
Figure 9. (a) X-ray diffractograms of CNNp; (b) X-ray diffractograms of CSNp.

3.6. UV-Visible Spectroscopy

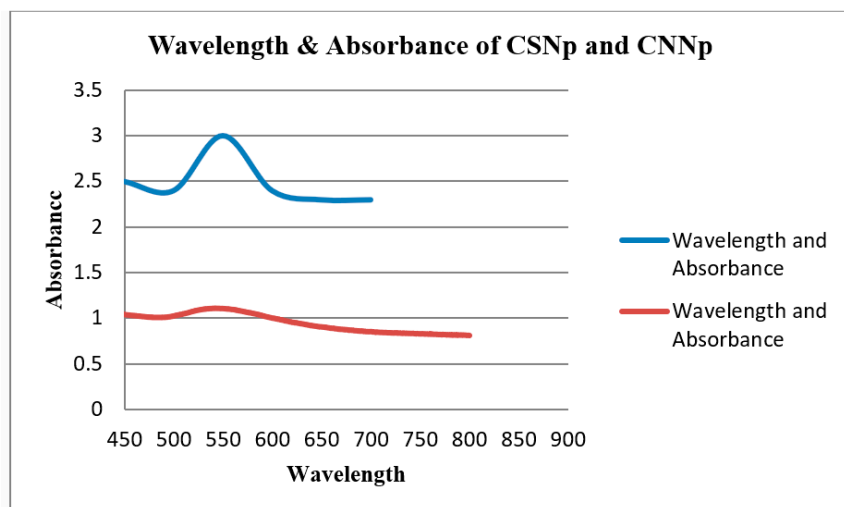
UV-Visible spectroscopy (UV-vis spectroscopy) was used to determine the absorbance of gold nanoparticles. In the process of the absorption and scattering of light by gold nanoparticles, the color change in this reaction was consistent with the occurrence of the maximum (λ_{\max}) of the localized surface plasmon resonance (LSPR) absorption band, which occurred in the range of 520–570 nm. The LSPR absorption bands of the green gold nanoparticles are shown in Table 2. The UV-Vis spectra of gold nanoparticles are shown in Figure 10a–c.



(a)



(b)



(c)

Figure 10. (a) UV-Vis spectra of CNNp; (b) UV-Vis spectra of CSNp; (c) UV-Vis spectra of CSNp and CNNp. Blue line and red line show CSNp and CNNp, respectively.

Table 2. Maximum value of localized surface plasmon resonance (LSPR) absorption band of prepared green gold nanoparticles.

Plants	Reducing Agent	Concentration (mg/100 μ L)	λ_{\max} (nm)
<i>Camellia sinensis</i>	<i>Camellia sinensis</i> leaves extract	3.9	550
<i>Cocos nucifera</i>	<i>Cocos nucifera</i> water	3.9	535

3.7. Antimicrobial Activity

Zone of inhibition:

The zones of inhibition of CSE, CNW and gold nanoparticles were calculated against the pathogenic bacteria *Staphylococcus aureus*. The zones of inhibition are shown in Figure 11a,b.

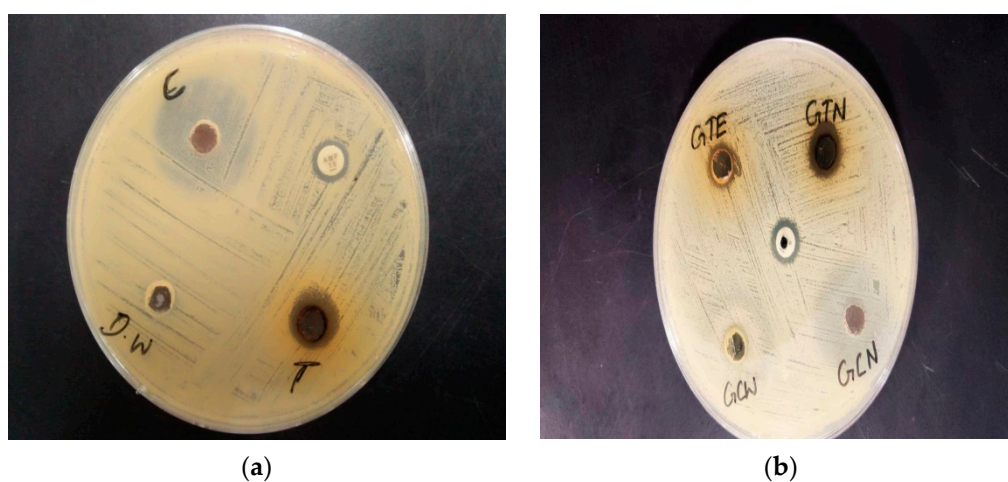


Figure 11. (a) Zones of inhibition of CSNp and CNNp against *Staphylococcus aureus*; (b) zones of inhibition of CSE, CNW, CSNp and CNNp against *Staphylococcus aureus*. C: Green coconut (*Cocos nucifera*) gold nanoparticles; T: green tea (*Camellia sinensis*) gold nanoparticles; Amp: ampicillin (antibiotic); DW: distilled water; GTE: green tea (*Camellia sinensis*) extract; GTN: green tea (*Camellia sinensis*) gold nanoparticles; GCW: green coconut (*Cocos nucifera*) water; GCN: green coconut (*Cocos nucifera*) gold nanoparticles.

The zone of inhibition of CSNp was 13 mm; for CNNp, it was 25 mm; for ampicillin, it was 9 mm. There was not considered to be a zone of inhibition in the case of *Staphylococcus aureus*. The zone of inhibition for CSE was 10 mm, and for CSNp, it was 13 mm. The zone of inhibition for CNW was 22 mm, and for CNNp is 25 mm. This meant that gold nanoparticles displayed better results as compared to CSE and CNW.

3.8. Minimum Inhibitory Concentration (MIC)

MIC of CSNp for 24 h incubation:

The analysis of variance (Table 3) showed that the 24 h incubation of *Staphylococcus aureus* with CSNp had a significant effect on the OD value of the culture and thus on the growth of *Staphylococcus aureus* ($p < 0.05$). Different concentrations of CSNp were used to determine the MICs, which are shown in Tables 3 and 4.

Table 3. Analysis of variance for MICs of different concentrations of CSNp against *S. aureus* for 24 h incubation.

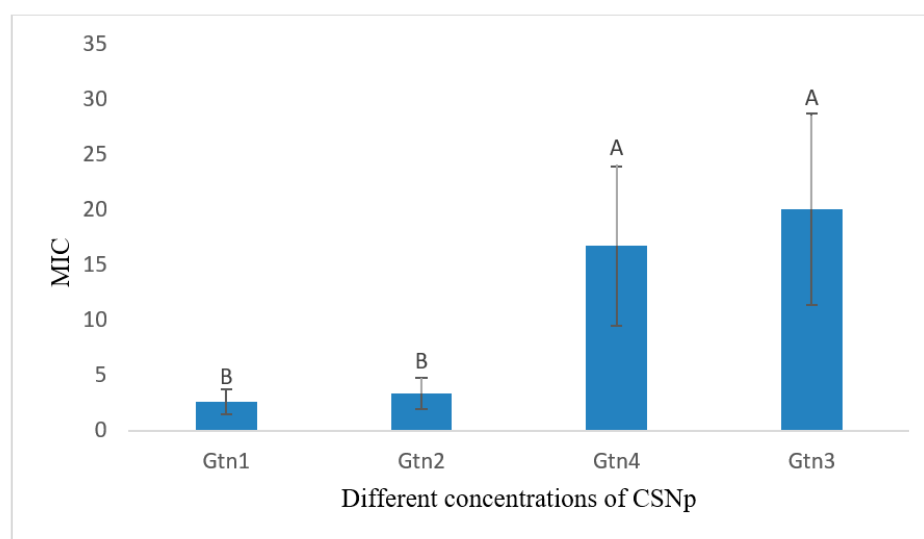
Analysis of Variance					
Source	DF	Adj SS	Adj MS	F-Value	p-Value
Factor	3	725.9	241.96	7.42	0.011
Error	8	260.9	32.61		
Total	11	986.7			

The comparison of the means showed significant differences among various test groups (Table 4). The lowest MIC was found in the case of GTN1 (2.600 ± 1.126^B $\mu\text{g}/\text{mL}$) for 24 h of incubation. The comparison of means showed GTN to be significantly lower ($p < 0.05$) as compared to GTN3 and GTN4, while with GTN2, it showed a non-significant difference ($p > 0.05$). On the other hand, the highest MIC was noted in the case of GTN3 (20.00 ± 8.66^A $\mu\text{g}/\text{mL}$). Graphical representation of mean MICs of concentrations of CSNp against the pathogen, *S. aureus* is shown in Figure 12.

Table 4. Comparison of mean MICs of different concentrations of CSNp against *S. aureus*.

Different Concentrations of CSNp	Mean \pm SD
GTN3 (30 mg/ μL)	20.00 ± 8.66^A
GTN4 (50 mg/ μL)	16.67 ± 7.22^A
GTN2 (10 mg/ μL)	3.333 ± 1.444^B
GTN1 (3.9 mg/ μL)	2.600 ± 1.126^B

Means that do not share A letter are significantly different.

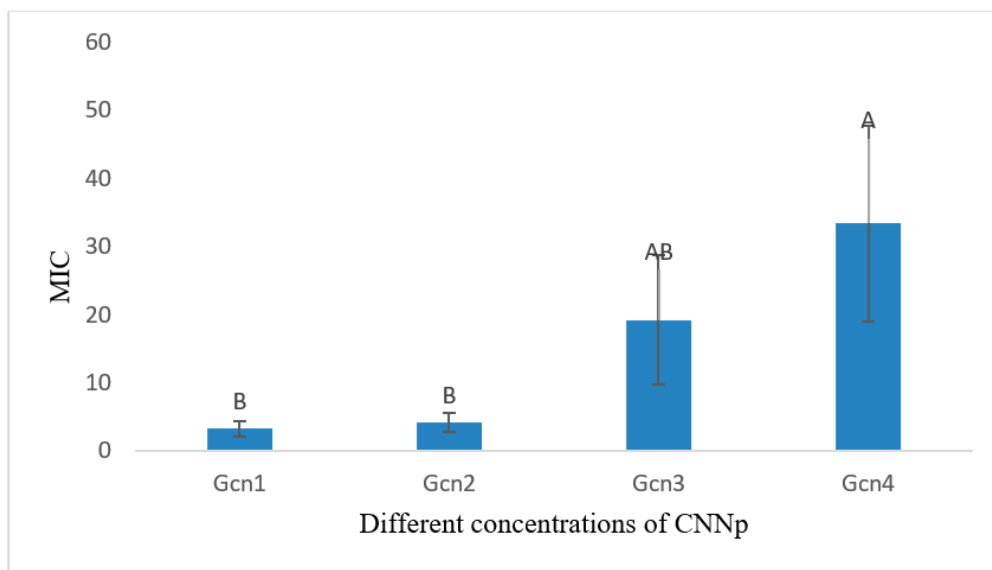
**Figure 12.** Graphical representation of mean MICs of different concentrations of CSNp against *S. aureus* for 24 h incubation. Means that do not share A letter are significantly different.

MIC of CNNp for 24 h incubation:

The analysis of variance (Table 5) showed that the 24 h incubation of *Staphylococcus aureus* with CNNp had a significant effect on the OD value of the culture and thus on the growth of *Staphylococcus aureus* ($p < 0.05$). Figure 13 is showing mean MIC values of different concentrations of CNNp against *S. aureus* after incubating for 24 h.

Table 5. Analysis of variance for MICs of different concentrations of CNNp against *S. aureus*.

Analysis of Variance					
Source	DF	Adj SS	Adj MS	F-Value	p-Value
Factor	3	1826.7	608.89	8.08	0.008
Error	8	602.5	75.32		
Total	11	2429.2			

Significant if p -value < 0.05**Figure 13.** Graphical representation of mean MICs of different concentrations of CNNp against *S. aureus* for 24 h of incubation. Means that do not share A letter are significantly different.

The comparison of means showed significant differences among various test groups (Table 6). The lowest MIC was found in the case of GCN1 (3.250 ± 1.126^B $\mu\text{g}/\text{mL}$) for 24 h of incubation. The comparison of means showed GCN1 to be significantly lower ($p < 0.05$) as compared to GCN4, while with all other preparations, it showed non-significant differences ($p > 0.05$). On the other hand, the highest MIC was noted in the case of GCN4 (33.33 ± 14.43^A $\mu\text{g}/\text{mL}$).

Table 6. Comparison of mean MICs of different concentrations of CNNp against *S. aureus* for 24 h of incubation.

Different Concentrations of CNNp	Mean \pm SD
GCN4 (50 mg/ μL)	33.33 ± 14.43^A
GCN3 (30 mg/ μL)	19.17 ± 9.46^{AB}
GCN2 (10 mg/ μL)	4.167 ± 1.443^B
GCN1 (3.9 mg/ μL)	3.250 ± 1.126^B

Means that do not share A letter are significantly different.

4. Discussion

Gold nanoparticles prepared using green plants do not require any external chemical agents for the reduction and stabilization of the nanoparticles. Phytochemical substances present in CNW or CSE are responsible for the formation of coatings on gold nanoparticles, and these nanoparticles are stable against agglomeration.

Nanoparticles have an extensive range of biological targets because of their smaller size, so the zeta size and zeta potential are the most important features of nanoformulations [17]. Zeta potential was used to determine the surface charge of nanoparticles. The zeta sizes of CSNp and CNNp were 41.61 nm and 34.12 nm. The zeta potential values of CSNp and CNNp were -16.52 mV and -14.61 mV. These results are aligned with [18,19].

UV-Visible spectroscopy was used to determine the absorbance of gold nanoparticles. The maximum (λ_{max}) of the localized surface plasmon resonance (LSPR) absorption band occurred in the range of 520–570 nm for gold nanoparticles. The λ_{max} of CSNp was 540 nm, and for CNNp, it was 524 nm. These conclusions are related to the conclusions in [20].

The peaks of the FTIR results confirmed that CSNp and CNNp both followed the same trends of peaks, which confirmed the preparation of green gold nanoparticles. These findings are similar to Ref. [21].

SEM gave information about the morphology of gold nanoparticles, which were spherical shapes; these observations are in agreement with Yadav et al., who prepared nanoparticles using *Camellia sinensis*. CSNp showed no agglomerates. TEM gave highly magnified images of gold nanoparticles which were prepared using CSE and CNW. These outcomes are similar the conclusions of Ref. [22].

The crystal structures of the gold nanoparticles were presented via XRD. The diffraction peaks of green tea gold nanoparticles were observed at 38.17° , 44.66° , 66.13° and 76.19° , representing the intensities of (353.11), (141.1), (137.37) and (131.14). The diffraction peaks of green coconut gold nanoparticles were observed at 38.88° , 43.46° , 64.19° and 78.99° , representing the intensities of (255.13), (98.12), (92.11) and (105.22), which describe the crystalline structures of gold nanoparticles; these conclusions are comparable with those in Ref. [23].

Using the well diffusion method on an agar plate, the antimicrobial actions of green gold nanoparticles with a size range between 30 and 80 nm were determined, and the zone of inhibition of *S. aureus* was observed. The well diffusion method results for CSNp and CNNp against *S. aureus* are shown in Figure 11a,b, which clearly show the zones of inhibition. Additionally, the zone of inhibition of CNNp was greater than that of CSNp. These conclusions are similar with the discussion of Ref. [24]. The MIC is the lowest concentration of antibacterial agents that inhibit the growth of bacteria via serial dilution. In Table 4, the MIC values of different concentrations of CSNp are shown. GTN1 (3.9 mg/ μL) had the lowest value of MIC, which was $(2.600 \pm 1.126^{\text{B}})$. In Table 6, the MIC values of different concentrations of CNNp are shown. GCN1 (3.9 mg/ μL) had the lowest value of MIC, which was $(3.250 \pm 1.126^{\text{B}})$. These findings are similar to Ref. [25].

5. Conclusions

Gold nanoparticles of different sizes and shapes were synthesized via CSE and CNW, which act as reducing and stabilizing agents without implicating different physical and chemical methods. Gold nanoparticles were prepared via a biological method. This method is simple, eco-friendly and cost-effective and gives monodisperse, functional gold nanoparticles. The confirmation of gold nanoparticles was carried out via UV-Vis spectroscopy, DLS, FTIR, SEM, TEM and XRD. *Camellia sinensis* provided the formation of more stable nanoparticles and offered a wide range of particle sizes and shapes. In the current study, green gold nanoparticles showed excellent outcomes and maximum zones of inhibition against *S. aureus*. MICs were determined via the Broth Micro Dilution method against *S. aureus*. MIC outcomes were in accordance with the zone of inhibition; for example, the higher the zone of inhibition, the lower the MIC value, and vice versa.

Author Contributions: Conceptualization, S.A. (Sidra Altaf); methodology, S.A. (Saman Anwar) and S.A. (Sidra Altaf); software, S.A. (Saman Anwar), S.A. (Sidra Altaf) and M.S.U.R.B.; formal analysis, S.A. (Saman Anwar), S.A. (Sidra Altaf) and H.M.; investigation, S.A. (Saman Anwar), S.A. (Sidra Altaf), B.A., H.M. and A.I.; data curation, S.A. (Saman Anwar), S.A. (Sidra Altaf), H.M. and A.I.; writing—original draft preparation, S.A. (Saman Anwar) and M.S.U.R.B.; writing—review and editing, S.A. (Sidra Altaf), B.A., H.M. and A.I. All authors have read and agreed to the published version of the manuscript.

Funding: This research received no external funding.

Institutional Review Board Statement: The study was conducted in accordance with the Declaration of Helsinki, and approved by the Institutional Ethics committee of University of Agriculture, Faisalabad and initiated after issuance of bioethics certificate (Vide No. 1480/ORIC, Dated: 1 April 2021).

Informed Consent Statement: Not applicable.

Data Availability Statement: Not applicable.

Conflicts of Interest: The authors declare no conflict of interest.

Abbreviations

CSE, *Camellia sinensis* extract; CNW, *Cocos nucifera* water; CSNp, *Camellia sinensis* gold nanoparticle; CNNp, *Cocos nucifera* gold nanoparticle; A, ampicillin.

References

1. Steinig, E.J.; Duchene, S.; Robinson, D.A.; Monecke, S.; Yokoyama, M.; Laabei, M.; Slickers, P.; Andersson, P.; Williamson, D.; Kearns, A.; et al. Evolution and global transmission of a multidrug-resistant, community-associated methicillin-resistant staphylococcus aureus lineage from the Indian subcontinent. *MBio* **2019**, *10*, e01105-19. [[CrossRef](#)] [[PubMed](#)]
2. O'Malley, S.M.; Emele, F.E.; Nwaokorie, F.O.; Idika, N.; Umezudike, A.K.; Emeka-Nwabunnia, I.; Hanson, B.M.; Nair, R.; Wardyn, S.E.; Smith, T.C. Molecular typing of antibiotic-resistant Staphylococcus aureus in Nigeria. *J. Infect. Public Health* **2015**, *8*, 187–193. [[CrossRef](#)] [[PubMed](#)]
3. Paharik, A.E.; Parlet, C.P.; Chung, N.; Todd, D.A.; Rodriguez, E.I.; Van Dyke, M.J.; Cech, N.B.; Horswill, A.R. Coagulase-Negative Staphylococcal Strain Prevents Staphylococcus aureus Colonization and Skin Infection by Blocking Quorum Sensing. *Cell Host Microbe* **2017**, *22*, 746–756.e5. [[CrossRef](#)] [[PubMed](#)]
4. Aslam, B.; Arshad, M.I.; Aslam, M.A.; Muzammil, S.; Siddique, A.B.; Yasmeen, N.; Khurshid, M.; Rasool, M.; Ahmad, M.; Rasool, M.H.; et al. Bacteriophage Proteome: Insights and Potentials of an Alternate to Antibiotics. *Infect. Dis. Ther.* **2021**, *10*, 1171–1193. [[CrossRef](#)] [[PubMed](#)]
5. Aggarwal, S.; Jena, S.; Panda, S.; Sharma, S.; Dhawan, B.; Nath, G.; Singh, N.P.; Nayak, K.C.; Singh, D.V. Antibiotic Susceptibility, Virulence Pattern, and Typing of Staphylococcus aureus Strains Isolated From Variety of Infections in India. *Front. Microbiol.* **2019**, *10*, 2763. [[CrossRef](#)]
6. Gour, A.; Jain, N.K. Advances in green synthesis of nanoparticles. *Artif. Cells Nanomed. Biotechnol.* **2019**, *47*, 844–851. [[CrossRef](#)]
7. Akhtar, B.; Muhammad, F.; Aslam, B.; Saleemi, M.K.; Sharif, A. Pharmacokinetic profile of chitosan modified poly lactic co-glycolic acid biodegradable nanoparticles following oral delivery of gentamicin in rabbits. *Int. J. Biol. Macromol.* **2020**, *164*, 1493–1500. [[CrossRef](#)]
8. Salem, S.S.; Fouda, A. Green Synthesis of Metallic Nanoparticles and Their Prospective Biotechnological Applications: An Overview. *Biol. Trace Elem. Res.* **2021**, *199*, 344–370. [[CrossRef](#)]
9. Muhammad, F.; Nguyen, T.D.T.; Raza, A.; Akhtar, B.; Aryal, S. A review on nanoparticle-based technologies for biodegradation. *Drug Chem. Toxicol.* **2017**, *40*, 489–497. [[CrossRef](#)]
10. Gerald, A.N.; da Silva, A.A.; Leal, J.; Estrada-Villegas, G.M.; Lincopan, N.; Katti, K.V.; Lugatildeo, A.B. Green Nanotechnology from Plant Extracts: Synthesis and Characterization of Gold Nanoparticles. *Adv. Nanoparticles* **2016**, *5*, 176–185. [[CrossRef](#)]
11. Moongraksathum, B.; Chen, Y.W. Anatase TiO₂ co-doped with silver and ceria for antibacterial application. *Catal. Today* **2018**, *310*, 68–74. [[CrossRef](#)]
12. Ganachari, S.V.; Yaradoddi, J.S.; Somappa, S.B.; Mogre, P.; Tapaskar, R.P.; Salimath, B.; Venkataraman, A.; Viswanath, V.J. Green nanotechnology for biomedical, food, and agricultural applications. In *Handbook of Ecomaterials*; Springer International Publishing: Berlin/Heidelberg, Germany, 2019; Volume 4, pp. 2681–2698. ISBN 9783319682556.
13. Katas, H.; Moden, N.Z.; Lim, C.S.; Celesistinus, T.; Chan, J.Y.; Ganasan, P.; Suleman Ismail Abdalla, S. Biosynthesis and Potential Applications of Silver and Gold Nanoparticles and Their Chitosan-Based Nanocomposites in Nanomedicine. *J. Nanotechnol.* **2018**, *2018*, 4290705. [[CrossRef](#)]

14. Manandhar, S.; Luitel, S.; Dahal, R.K. In Vitro Antimicrobial Activity of Some Medicinal Plants against Human Pathogenic Bacteria. *J. Trop. Med.* **2019**, *2019*, 1895340. [[CrossRef](#)] [[PubMed](#)]
15. Shamaila, S.; Zafar, N.; Riaz, S.; Sharif, R.; Nazir, J.; Naseem, S. Gold nanoparticles: An efficient antimicrobial agent against enteric bacterial human pathogen. *Nanomaterials* **2016**, *6*, 71. [[CrossRef](#)]
16. Elbehiry, A.; Al-Dubaib, M.; Marzouk, E.; Moussa, I. Antibacterial effects and resistance induction of silver and gold nanoparticles against *Staphylococcus aureus*-induced mastitis and the potential toxicity in rats. *Microbiologyopen* **2019**, *8*, 698. [[CrossRef](#)] [[PubMed](#)]
17. Bhattacharjee, S. DLS and zeta potential—What they are and what they are not? *J. Control. Release* **2016**, *235*, 337–351. [[CrossRef](#)]
18. Yaqoob, S.B.; Adnan, R.; Rameez Khan, R.M.; Rashid, M. Gold, Silver, and Palladium Nanoparticles: A Chemical Tool for Biomedical Applications. *Front. Chem.* **2020**, *8*, 376. [[CrossRef](#)]
19. Anwar, M.; Muhammad, F.; Aslam, B.; Saleemi, M.K. Isolation, characterization and in-vitro antigenicity studies of outer membrane proteins (OMPs) of *Salmonella gallinarum* coated gold nanoparticles (AuNPs). *Immunobiology* **2021**, *226*, 152131. [[CrossRef](#)]
20. ElMitwalli, O.S.; Barakat, O.A.; Daoud, R.M.; Akhtar, S.; Henari, F.Z. Green synthesis of gold nanoparticles using cinnamon bark extract, characterization, and fluorescence activity in Au/eosin Y assemblies. *J. Nanoparticle Res.* **2020**, *22*, 309. [[CrossRef](#)]
21. Clarence, P.; Luvankar, B.; Sales, J.; Khusro, A.; Agastian, P.; Tack, J.C.; Al Khulaifi, M.M.; AL-Shwaiman, H.A.; Elgorban, A.M.; Syed, A.; et al. Green synthesis and characterization of gold nanoparticles using endophytic fungi *Fusarium solani* and its in-vitro anticancer and biomedical applications. *Saudi J. Biol. Sci.* **2020**, *27*, 706–712. [[CrossRef](#)]
22. Rodríguez-León, E.; Rodríguez-Vázquez, B.E.; Martínez-Higuera, A.; Rodríguez-Beas, C.; Larios-Rodríguez, E.; Navarro, R.E.; López-Esparza, R.; Iñiguez-Palomares, R.A. Synthesis of Gold Nanoparticles Using *Mimosa tenuiflora* Extract, Assessments of Cytotoxicity, Cellular Uptake, and Catalysis. *Nanoscale Res. Lett.* **2019**, *14*, 334. [[CrossRef](#)] [[PubMed](#)]
23. Doan, V.D.; Huynh, B.A.; Nguyen, T.D.; Cao, X.T.; Nguyen, V.C.; Nguyen, T.L.H.; Nguyen, H.T.; Le, V.T. Biosynthesis of Silver and Gold Nanoparticles Using Aqueous Extract of *Codonopsis pilosula* Roots for Antibacterial and Catalytic Applications. *J. Nanomater.* **2020**, *2020*, 8492016. [[CrossRef](#)]
24. Folorunso, A.; Akintelu, S.; Oyebamiji, A.K.; Ajayi, S.; Abiola, B.; Abdusalam, I.; Morakinyo, A. Biosynthesis, characterization and antimicrobial activity of gold nanoparticles from leaf extracts of *Annona muricata*. *J. Nanostructure Chem.* **2019**, *9*, 111–117. [[CrossRef](#)]
25. Loo, Y.Y.; Rukayadi, Y.; Nor-Khaizura, M.A.R.; Kuan, C.H.; Chieng, B.W.; Nishibuchi, M.; Radu, S. In Vitro antimicrobial activity of green synthesized silver nanoparticles against selected Gram-negative foodborne pathogens. *Front. Microbiol.* **2018**, *9*, 1555. [[CrossRef](#)]

Disclaimer/Publisher's Note: The statements, opinions and data contained in all publications are solely those of the individual author(s) and contributor(s) and not of MDPI and/or the editor(s). MDPI and/or the editor(s) disclaim responsibility for any injury to people or property resulting from any ideas, methods, instructions or products referred to in the content.